

Electronic Supplementary Material (ESI) for Journal of Materials Chemistry A.
This journal is © The Royal Society of Chemistry 2016

Electronic Supplementary Information

High efficiency organic photovoltaic devices based on isoindigo conjugated polymers with a thieno[3,2-*b*]thiophene π -bridge

Lei Zhu,^a Min Wang,^a Bowen Li,^a Chao Jiang^{*b} and Qifang Li^{*a}

^a State Key Laboratory of Chemical Resource Engineering, College of Materials Science and Engineering, Beijing University of Chemical Technology, Beijing 100029, P. R. China. *E-mail: qflee@mail.buct.edu.cn

^b National Center for Nanoscience and Technology, Beijing 100190, P. R. China. *E-mail: jiangch@nanoctr.cn

Experimental Section

Instruments and Characterization: ^1H NMR (400 MHz) and ^{13}C NMR (100 MHz) spectra were acquired using a Bruker AV-400 MHz NMR spectrometer. Chemical shifts are reported in parts per million (ppm, δ). ^1H NMR and ^{13}C NMR spectra were referenced to tetramethylsilane (0 ppm) for CDCl_3 . The gel permeation chromatography (GPC) measurements were performed on Waters 1515-2414 with polystyrenes as a standard and THF as an eluent. Elemental analysis was performed on a vario EL CUBE elemental Analysensysteme. UV-vis absorption spectra were recorded on a Shimadzu spectrometer model UV-1800 with chloroform solutions or films on the quartz plates at room temperature. Thermal gravimetric analysis (TGA, Netzsch TG209C) measurements were carried out under a nitrogen atmosphere at the heating rate of 10 K min^{-1} . The atomic force microscopy (AFM) measurement of the surface morphology of samples was conducted on Dimension 3100 (Veeco, USA) in tapping mode. The sample films were prepared on quartz with the optimal condition. The morphologies of the nanostructures were characterized by transmission electron microscopy (TEM, Tecnai G2 F20 S-TWIN, FEI Co., USA). Cyclic voltammetry was performed on a CH-Instruments 650A electrochemical workstation in acetonitrile solutions at a scan rate of 50 mV s^{-1} . Glass carbon used as the working electrode, saturated calomel reference electrode (SCE) used as the reference electrode, and Pt wire used as the counter electrode. The supporting electrolyte was tetrabutylammonium hexafluorophosphate (Bu_4NPF_6 , 0.1 M) and ferrocene was selected as the internal standard. The solutions were bubbled with a constant nitrogen flow for 15 min before measurements.

Quantum chemical calculations: The density functional theory (DFT) calculations were performed by using Gaussian 09 package^[1] with hybrid B3LYP correlation functional and a split valence 6-31G (d, p) basis set. Molecular containing one repeat unit was taken as a model for calculations and methyl was used instead of long side chains.

Device Fabrication: Polymer solar cell devices with ITO/PEDOT:PSS/polymer:PC₇₁BM/Ca/Al structures were fabricated according to the following procedure. Patterned ITO glass substrates were first cleaned with detergent, and ultrasonicated in acetone, isopropyl alcohol, deionized water and finally ethanol for 10 min each and then dried under nitrogen. The precleaned substrates were treated in an ultraviolet-ozone chamber (Ultraviolet Ozone Cleaner, Jelight Company, USA) for 15 min, then a 45 nm thick PEDOT:PSS (Clevious P VP AI 4083 H. C. Stark, Germany) thin film was deposited onto the ITO surface layer by spin-coating and baked at 150 °C for 15 min. Subsequently, they were transferred to a glovebox for spin-coating the active layer and subsequent procedures. The blend solution of PBDT-TT-IID:PC₇₁BM (1:1.5, wt%, 4 mg mL⁻¹ for polymer) in 1,2-dichlorobenzene (DCB) with or without 3% diiodooctane (DIO) was stirred at 25 °C for eight hours in advance and then spin-coated on top of the PEDOT:PSS layer at a speed of 800 rpm for 60s. And the mixture of PBDTT-TT-IID:PC₇₁BM (1:5, wt %, 4 mg mL⁻¹ for polymer) in chloroform solvent with or without 3% DIO pre-stirred at 25 °C for two hours was dropped onto the PEDOT:PSS layer and spin-casted at 2500 rpm for 30s. The prepared films were treated with thermal annealing at 50 °C for 10 min on the hot plate in the glove box. For the methanol treated device, methanol was spin-coated on the active layer at 3000 rpm for 40s. The thickness of the active layer was measured by KLA Tencor D-120 profilometer. Those samples were brought into to an evaporate chamber and a 20 nm thick calcium (Ca) layer was thermally evaporated on the active layer followed by a 100 nm aluminum (Al) electrode was deposited at a base pressure of 10⁻⁶ mbar. The evaporation thickness was controlled by SQC-310C deposition controller (INFICON, Germany). Four devices were fabricated on one substrate and the active area of each device was 4.000 mm² defined by a shadow mask.

The current-voltage (*J-V*) curves were measured with Keithley 236 Source under the illumination of AM 1.5 G irradiation (100 mW cm⁻²) using a 150 W solar simulator (Oriel

91159A, Newport, USA.) in ambient air. The light intensity was determined by a $2 \times 2 \text{ cm}^2$ standardized monosilicon cell (Oriental PN 91150V, Newport, USA.) calibrated by the National Renewable Energy Laboratory (NREL). The external quantum efficiency (EQE) measurement was conducted on a TRACQ-BASIC System using a lock-in amplifier with a monochromator and 500 W xenon lamp. A calibrated silicon detector (PRL-12, Newport, USA) with known photo response was utilized as a reference.

The hole-only devices were fabricated with ITO/PEDOT:PSS/polymer:PC₇₁BM/Au (80 nm) structures applying the same processes with the photovoltaic devices. The space charge limited current (SCLC) mobility was calculated according to the Mott-Gurney square law $J = 9\epsilon_r\epsilon_0\mu_h V^2/8L^3$,^[2] where J is the current density, ϵ_r is relative permittivity of the polymer, ϵ_0 is the vacuum permittivity, μ_h is the hole mobility, V is the applied voltage, and L is the thickness of active layer. The electron-only devices were fabricated with Al (80 nm)/polymer:PC₇₁BM/Al (80 nm) structures. The space charge limited current (SCLC) mobility was calculated according to the Mott-Gurney square law $J = 9\epsilon_r\epsilon_0\mu_e V^2/8L^3$, where J is the current density, ϵ_r is relative permittivity of the PC₇₁BM, ϵ_0 is the vacuum permittivity, μ_e is the electron mobility, V is the applied voltage, and L is the thickness of active layer.

Table S1. Calculated dihedral angles, bond angle and corresponding HOMO, LUMO levels and bandgaps (E_g^{cal}) of the polymers.

Polymer	Dihedral angle (°)			Bond angle (°)	HOMO (eV)	LUMO (eV)	E_g^{cal} (eV)
	A1 ^a	A2 ^a	A3 ^a	A4 ^a			
PBDT-TT-IID	-34.05	22.09	23.23	183.34	-5.08	-2.84	2.24
PBDTT-TT-IID	-32.72	-23.09	-23.66	176.69	-5.01	-2.82	2.19

^a The corresponding relation of each angle as shown in the figure below

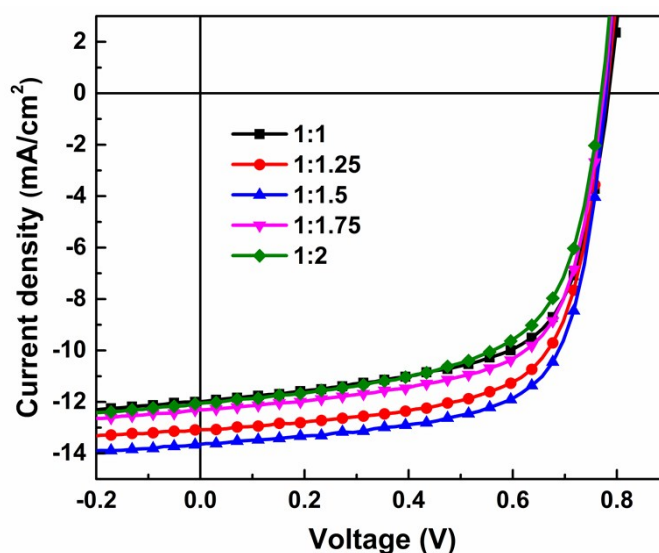
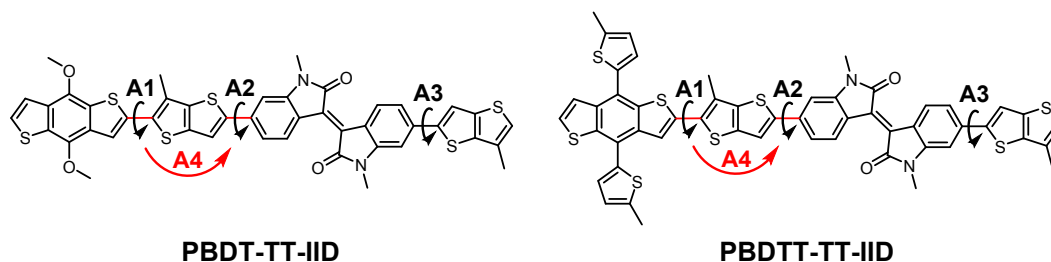


Fig. S1 J - V curves of PSCs based on PBDTT-TT-IID:PC₇₁BM (chloroform with 3% DIO) with different D/A ratio.

Table S2. Photovoltaic characteristics of the devices based on PBDTT-TT-IID:PC₇₁BM with different D/A ratio. (The data in bracket were the best value)

Ratio	V_{oc} (V)	J_{sc} (mA/cm ²)	FF	PCE (%)	Thickness (nm)
1:1	0.78±0.01 (0.78)	11.68±0.21 (11.95)	0.64±0.01 (0.64)	5.84±0.17 (6.02)	105
1:1.25	0.77±0.01 (0.78)	12.72±0.30 (13.07)	0.66±0.01 (0.67)	6.58±0.19 (6.79)	100
1:1.5	0.77±0.01 (0.77)	13.33±0.26 (13.64)	0.68±0.01 (0.68)	6.99±0.21 (7.20)	100
1:1.75	0.76±0.01 (0.77)	12.04±0.22 (12.31)	0.65±0.01 (0.66)	6.04±0.15 (6.22)	105
1:2	0.77±0.01 (0.77)	11.84±0.18 (12.05)	0.62±0.01 (0.62)	5.51±0.22 (5.75)	100

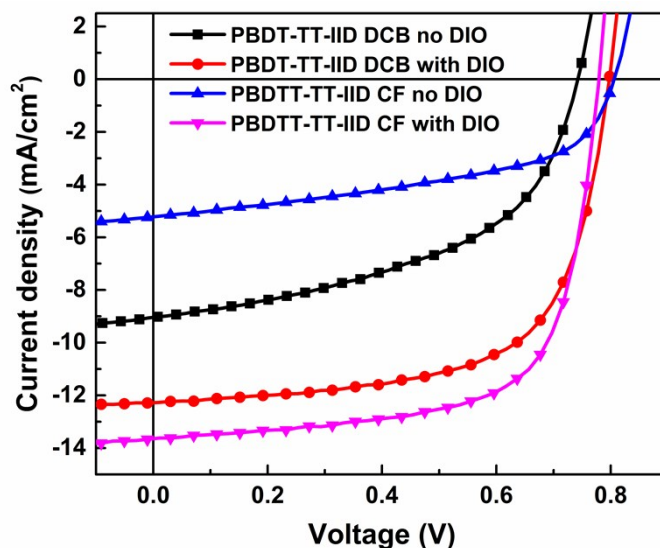


Fig. S2 J - V curves of PSCs based on polymers:PC₇₁BM (1:1.5) with different solvents.

Table S3. Photovoltaic characteristics of the devices based on polymers:PC₇₁BM with different solvents. (The data in bracket were the best value)

Polymer	Solvent	V_{oc} (V)	J_{sc} (mA/cm ²)	FF	PCE (%)	Thickness (nm)
PBDT-TT-IID	DCB	0.71±0.03 (0.73)	8.66±0.36 (9.04)	0.50±0.02 (0.51)	3.06±0.29 (3.37)	105
	DCB+3% DIO	0.79±0.01 (0.79)	12.09 ±0.12 (12.24)	0.64±0.01 (0.65)	6.26±0.08 (6.31)	100
PBDTT-TT-IID	CF	0.78±0.02 (0.80)	4.86±0.32 (5.22)	0.48±0.02 (0.50)	1.71±0.39 (2.09)	100
	CF+3% DIO	0.77±0.01 (0.77)	13.33±0.26 (13.64)	0.68±0.01 (0.68)	6.99±0.21 (7.20)	100

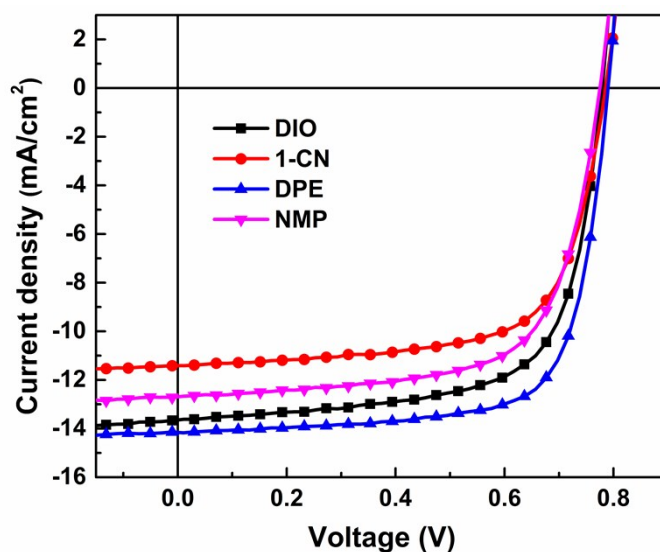


Fig. S3 J - V curves of PSCs based on PBDTT-TT-IID:PC₇₁BM (1:1.5) with different solvent additives.

Table S4. Photovoltaic characteristics of the devices based on PBDTT-TT-IID:PC₇₁BM with different solvent additives. (The data in bracket were the best value)

Solvents	V_{oc} (V)	J_{sc} (mA/cm ²)	FF	PCE (%)	Thickness (nm)
CF+3% DIO	0.77±0.01 (0.77)	13.33±0.26 (13.64)	0.68±0.01 (0.68)	6.99±0.21 (7.20)	100
CF+3% 1-CN	0.78±0.01 (0.78)	11.19±0.18 (11.40)	0.68±0.01 (0.68)	5.85±0.17 (6.05)	105
CF+3% DPE	0.79±0.01 (0.79)	13.96±0.15 (14.14)	0.72±0.01 (0.72)	7.88±0.13 (8.05)	100
CF+3% NMP	0.77±0.01 (0.77)	12.48±0.16 (12.68)	0.66±0.01 (0.67)	6.43±0.12 (6.58)	100

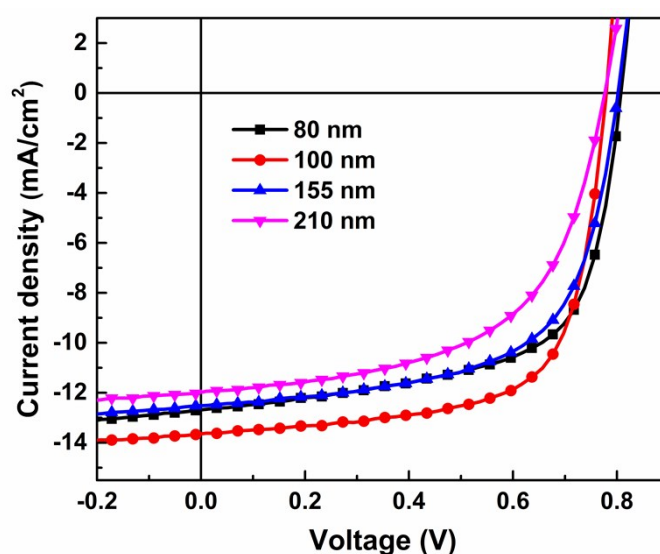


Fig. S4 J - V curves of PSCs based on PBDTT-TT-IID:PC₇₁BM (1:1.5) with different active layer thicknesses.

Table S5. Photovoltaic characteristics of the devices based on PBDTT-TT-IID:PC₇₁BM with different active layer thicknesses. (The data in bracket were the best value)

Thickness (nm)	V_{oc} (V)	J_{sc} (mA/cm ²)	FF	PCE (%)
80	0.79±0.01 (0.80)	12.44±0.18 (12.67)	0.63±0.01 (0.64)	6.31±0.17 (6.52)
100	0.77±0.01 (0.77)	13.33±0.26 (13.64)	0.68±0.01 (0.68)	6.99±0.21 (7.20)
155	0.78±0.01 (0.80)	12.25±0.21 (12.51)	0.62±0.01 (0.62)	5.98±0.26 (6.25)
210	0.76±0.01 (0.77)	11.66±0.27 (11.96)	0.56±0.01 (0.57)	5.01±0.27 (5.31)

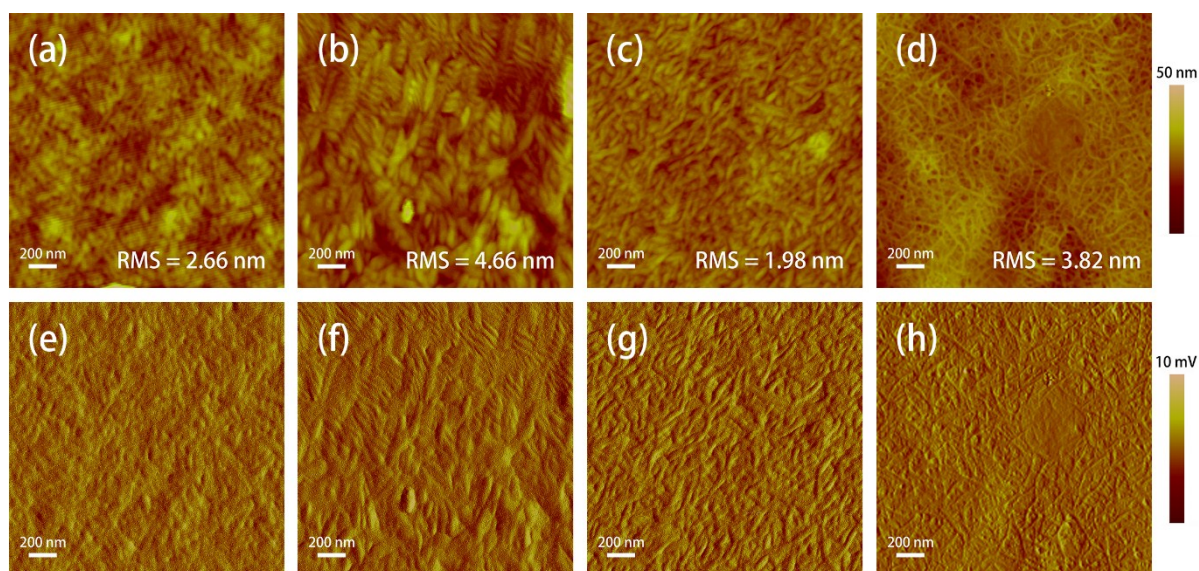
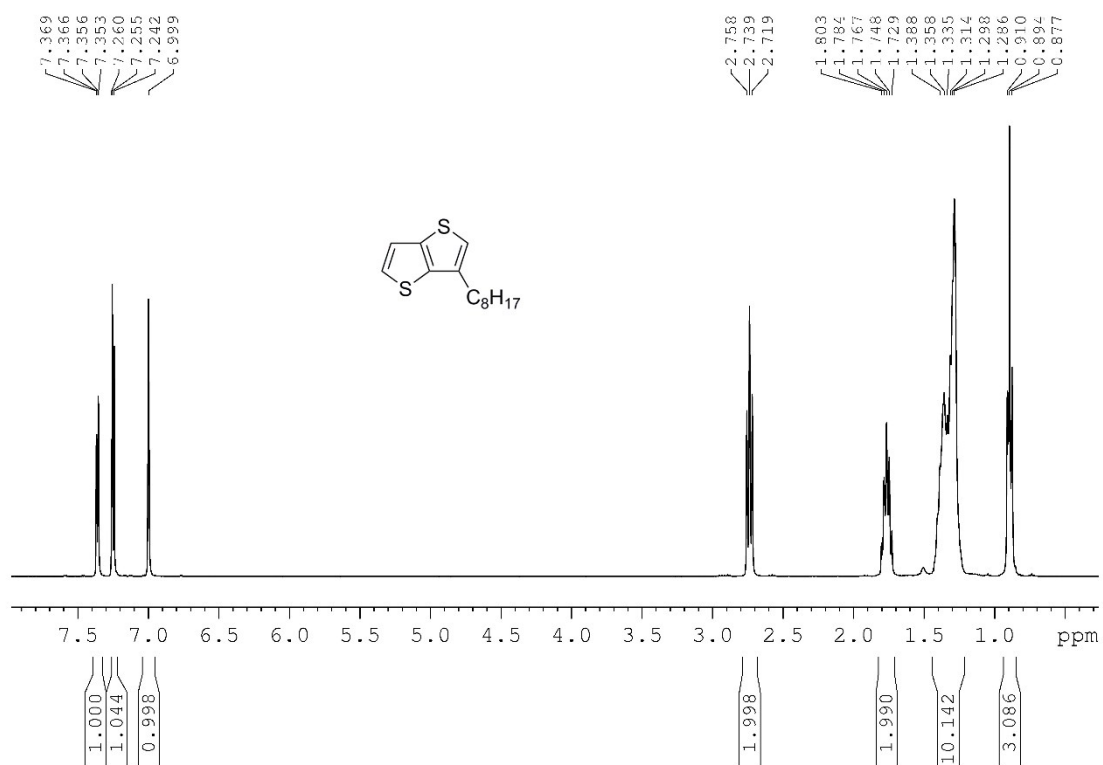
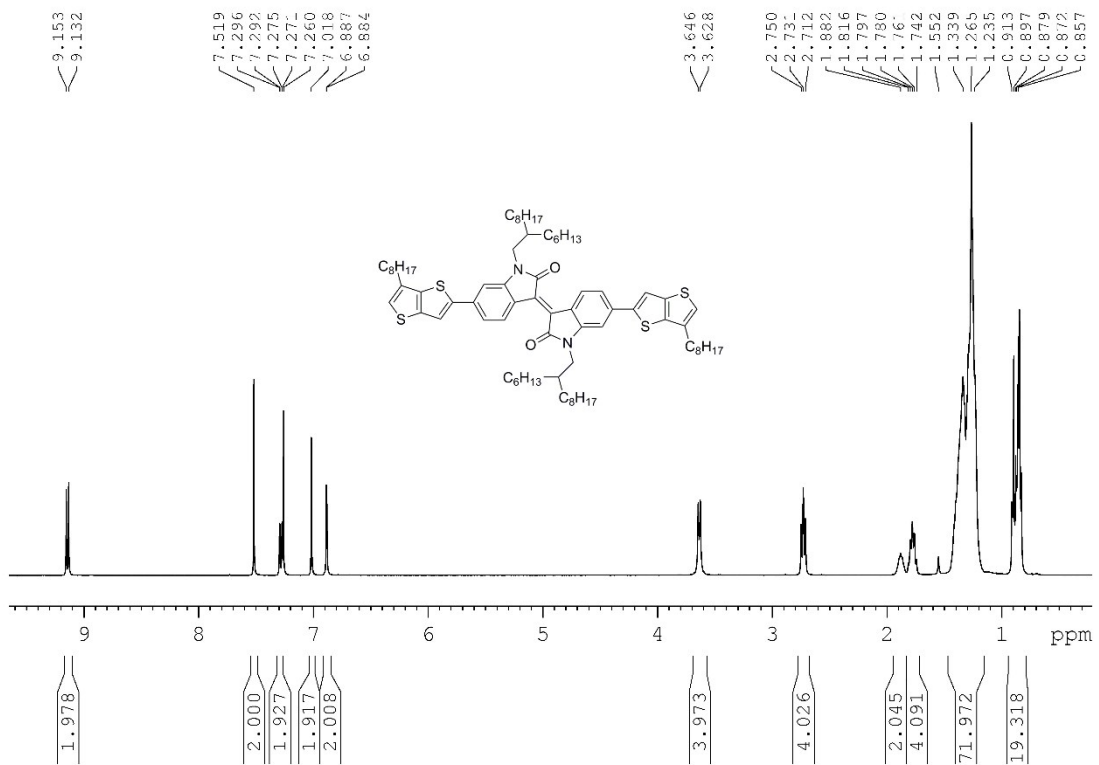
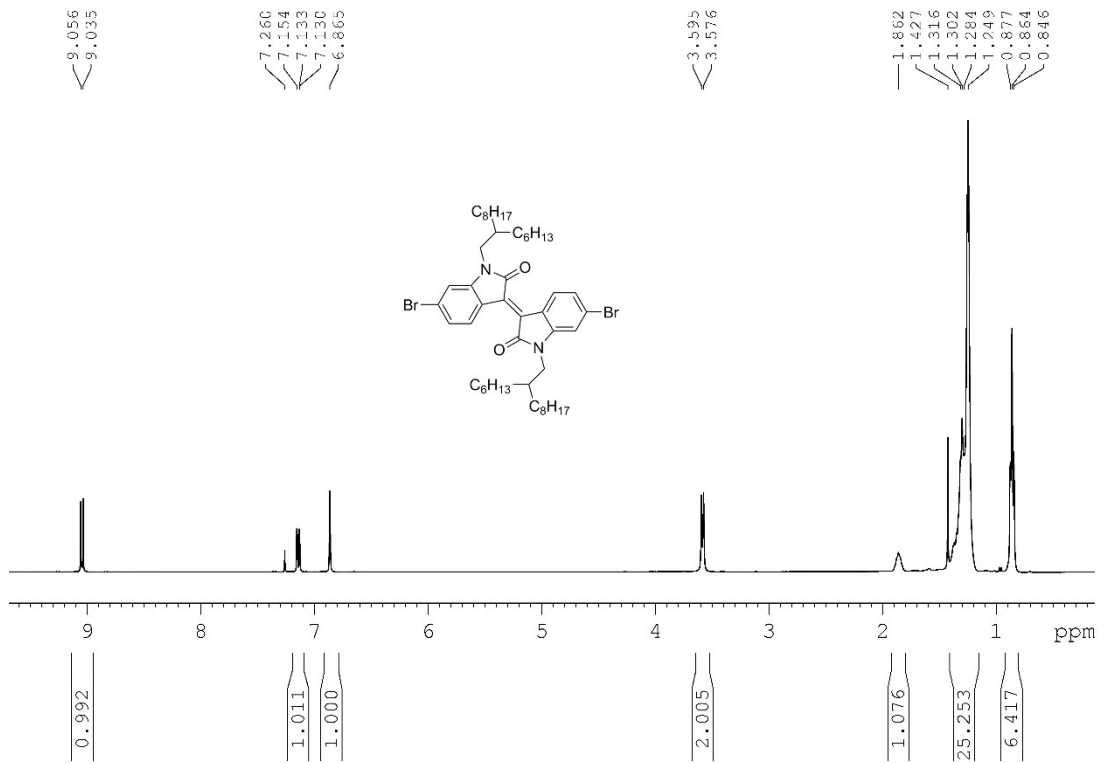


Fig. S5 AFM height images (top) and phase images (bottom) of PBDTT-TT-IID:PC₇₁BM blend films with with 3 vol% DIO (a and e), 3 vol% 1-CN (b and f), 3 vol% DPE (c and g) and 3 vol% NMP (d and h).





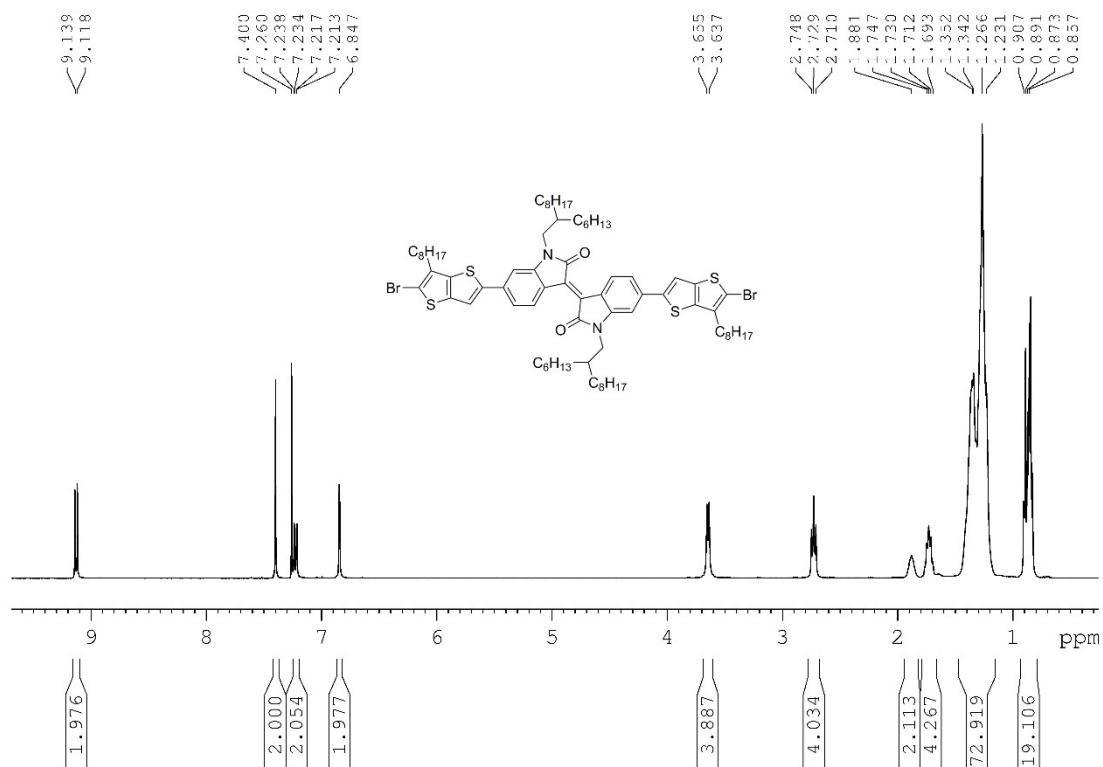
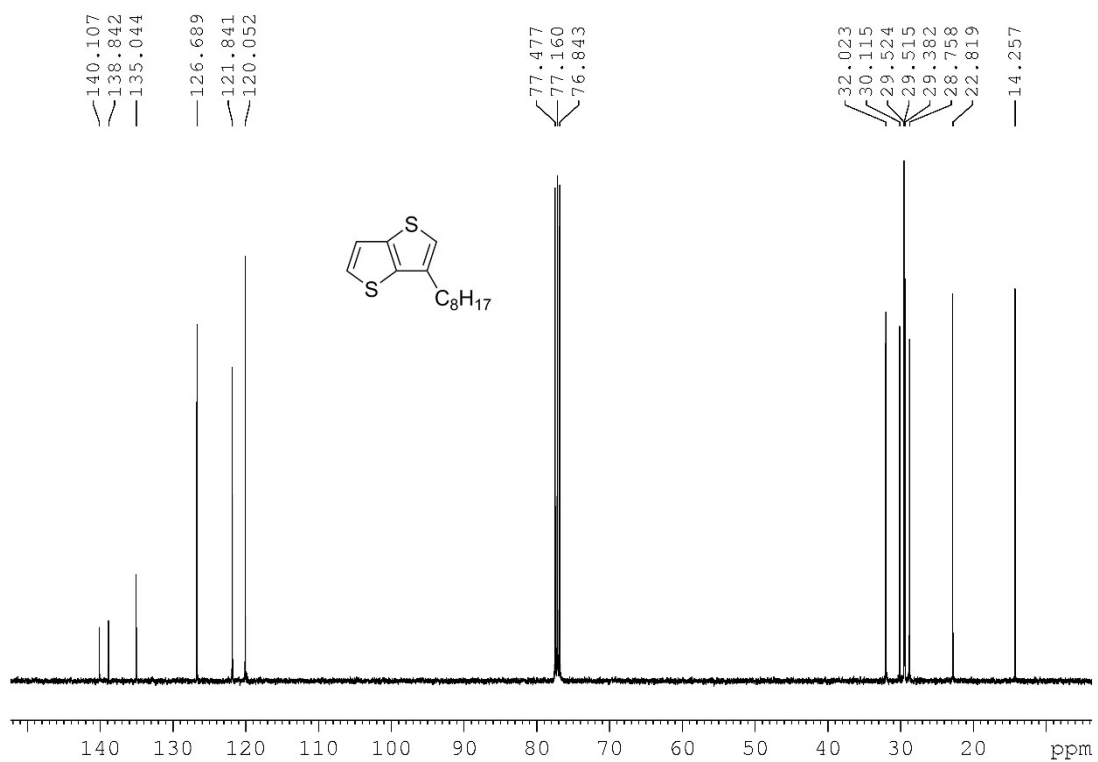
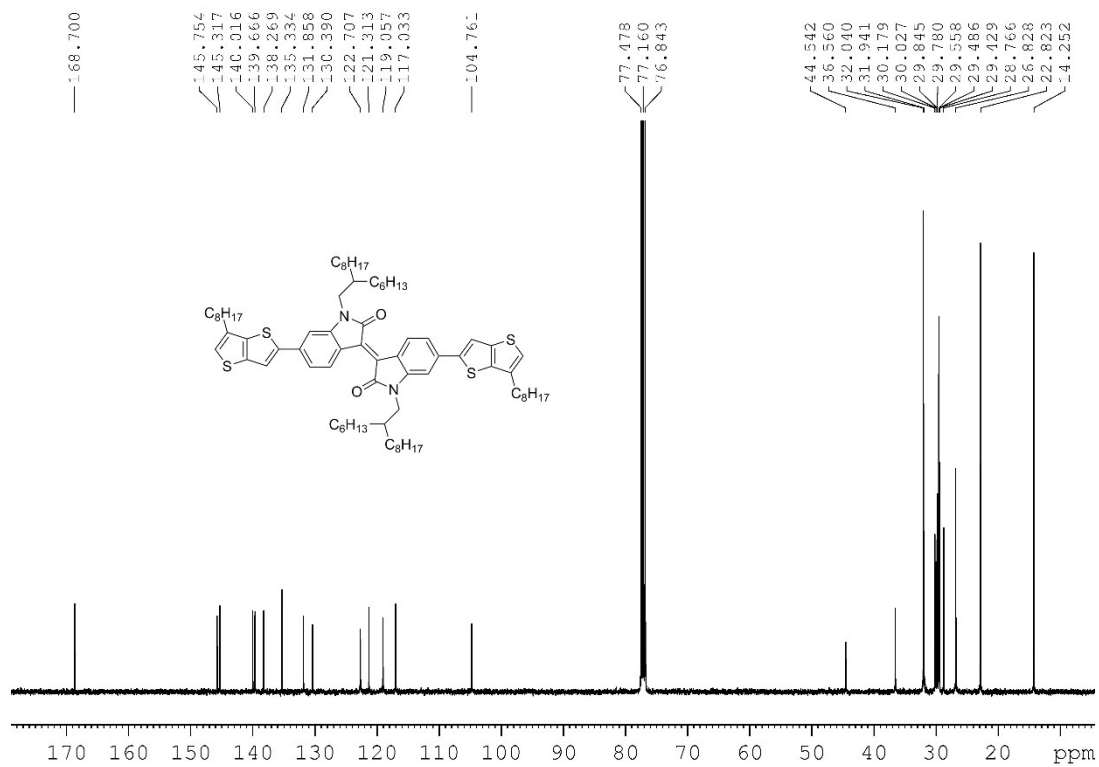
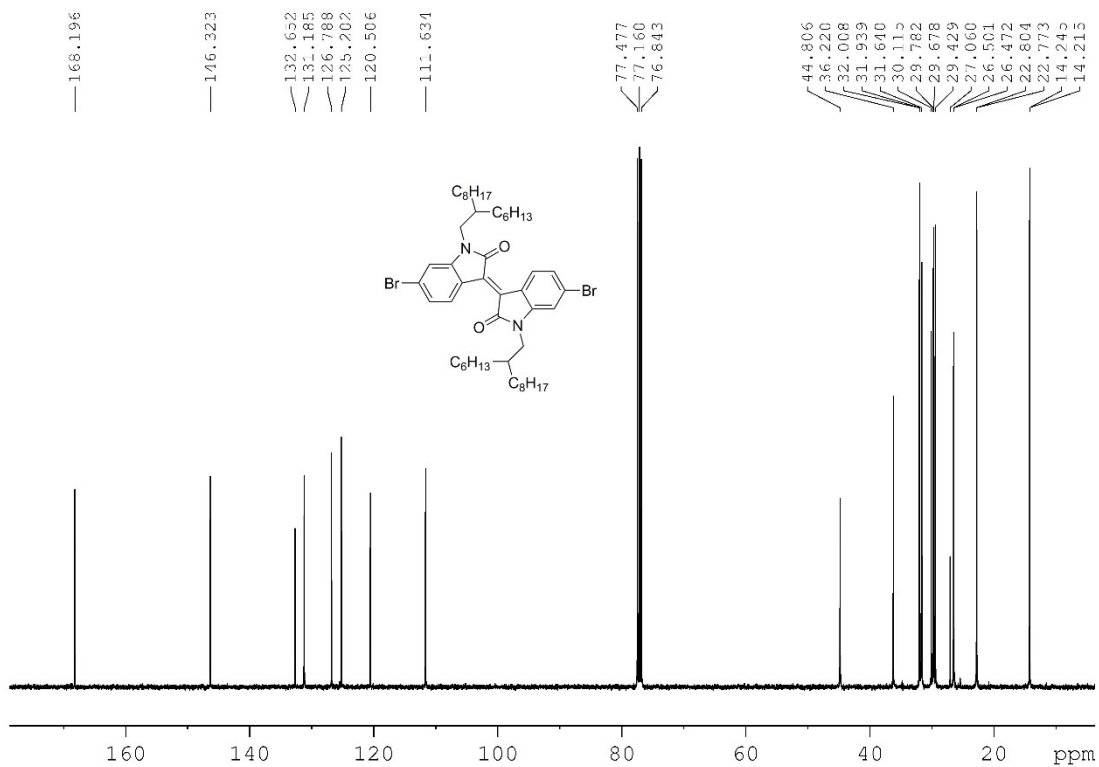


Fig. S6 ¹H NMR spectra of the monomers.





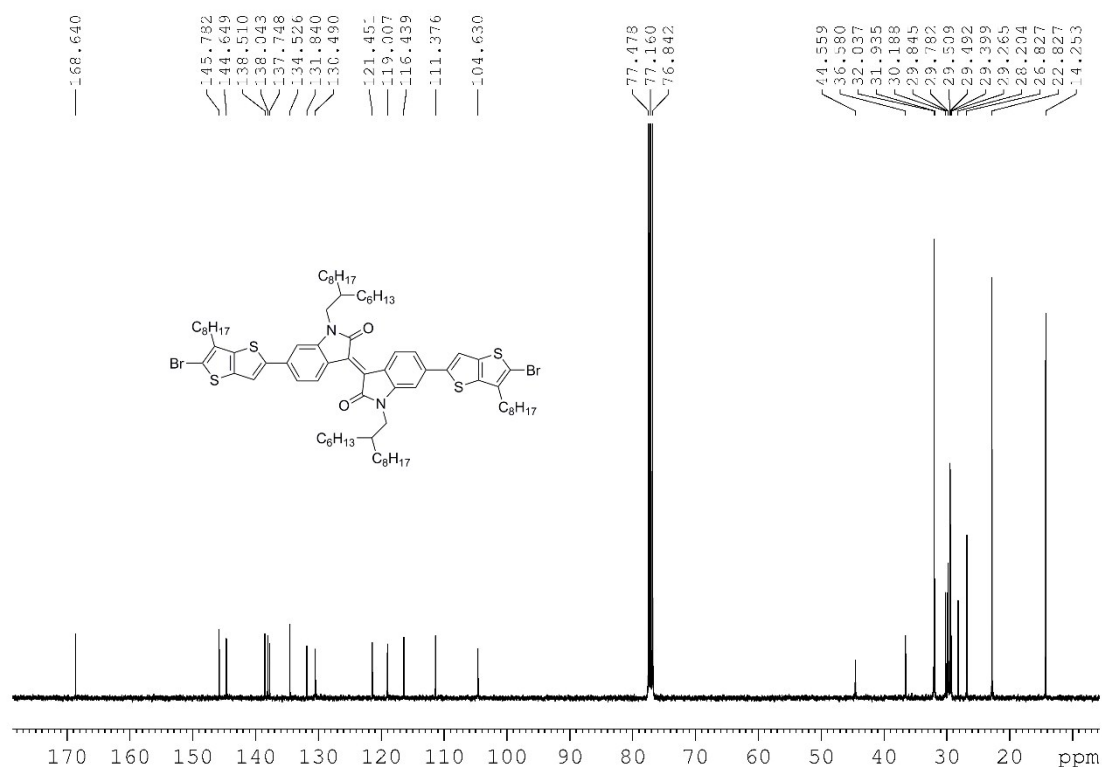


Fig. S7 ¹³C NMR spectra of the monomers.

References

- [1] M. J. Frisch, G. W. Trucks, H. B. Schlegel, G. E. Scuseria, M. A. Robb, J. R. Cheeseman, G. Scalmani, V. Barone, B. Mennucci, G. A. Petersson, H. Nakatsuji, M. Caricato, X. Li, H. P. Hratchian, A. F. Izmaylov, J. Bloino, G. Zheng, J. L. Sonnenberg, M. Hada, M. Ehara, K. Toyota, R. Fukuda, J. Hasegawa, M. Ishida, T. Nakajima, Y. Honda, O. Kitao, H. Nakai, T. Vreven, J. A. Montgomery, Jr., J. E. Peralta, F. Ogliaro, M. Bearpark, J. J. Heyd, E. Brothers, K. N. Kudin, V. N. Staroverov, R. Kobayashi, J. Normand, K. Raghavachari, A. Rendell, J. C. Burant, S. S. Iyengar, J. Tomasi, M. Cossi, N. Rega, J. M. Millam, M. Klene, J. E. Knox, J. B. Cross, V. Bakken, C. Adamo, J. Jaramillo, R. Gomperts, R. E. Stratmann, O. Yazyev, A. J. Austin, R. Cammi, C. Pomelli, J. W. Ochterski, R. L. Martin, K. Morokuma, V. G. Zakrzewski, G. A. Voth, P. Salvador, J. J. Dannenberg, S. Dapprich, A. D. Daniels, Ö. Farkas, J. B. Foresman, J. V. Ortiz, J. Cioslowski, D. J. Fox, *Gaussian, Inc., Wallingford CT*, **2009**.
- [2] H. T. Nicolai, G. A. H. Wetzelaer, M. Kuik, A. J. Kronemeijer, B. de Boer, P. W. M. Blom, *Appl. Phys. Lett.* **2010**, *96*.